RSC Advances

ROYAL SOCIETY OF CHEMISTRY

www.rsc.org/advances

Recyclable CuO nanoparticles as heterogeneous catalyst for the synthesis of xanthenes under solvent free conditions

Ganga Ram Chaudhary*, Pratibha Bansal, Navneet Kaur, S.K. Mehta

Department of Chemistry & Centre of Advanced Studies in Chemistry, Panjab University, Chandigarh - 160014, India

*Corresponding author. Tel.: +91-172 2534406; Fax: +91-172-2545074

E-mail address: grc22@pu.ac.in (Ganga Ram Chaudhary)

Abstract

CuO nanoparticles (NPs) of 17-22 nm size have been synthesized in very high yield in 4 minutes using microwave and water as medium. The obtained NPs have been characterized by FTIR, XRD and TEM. CuO NPs have been used as a nanocatalyst to carry out synthesis of xanthenes in solvent free conditions. They exhibit good catalytic activity with excellent yield. The main features of CuO NPs as catalyst in synthesis of xanthenes are reduced reaction time, higher yields, ease of product isolation, economic availability of catalyst, simple procedure, and no harmful byproduct. The spent heterogeneous catalyst have been recovered by simple filtration and reused for multiple cycles.

Keywords: CuO nanoparticles, Heterogeneous catalyst, xanthenes

1. Introduction

Nanoparticles (NPs) have received significant attention as efficient catalysts in many organic reactions due to their high surface-to-volume ratio and coordination parts which provide a larger number of active sites per unit area in comparison with their heterogeneous counter sites.[1] In the present report we have explored CuO (NPs) as catalyst.

Organic transformations using heterogeneous catalyst under solvent free condition has gained great importance, due to minimum pollution and easy work up conditions.[2-5] In recent years, much attention has been given to the synthesis of xanthene derivatives.[6-8]

Xanthenes and its derivatives are very important class of heterocyclic compounds because of their wide range of biological and pharmaceutical properties.[9] In addition, these compounds are widely used as dyes,[10] fluorescent materials for sensing of biomolecules[11] and for antiviral activity.[12] These compounds are also utilized as antagonists for paralyzing action of zoxazolamine and in photodynamic therapy.[13] Due to their wide range of applications, a wide variety of methods for the preparation of the xanthenes have been reported. Instead of Lewis acid[14-17] as catalyst, which is associated with harsh experimental conditions such as anhydrous condition, high temperature, prolonged reaction time, expensive, harmful and difficult to handle reagents, low yield, difficult work up, use of nanocatalyst has been encouraged in recent times.[18,19] There are successful attempts of xanthenes synthesis using ZnO[18] and Fe_3O_4 nanocatalyst.[19] However, in both cases quantity of catalyst required is large, moreover it takes more time to produce xanthenes with lesser yield.

Among various metal oxides NPs, in the present study we have choosen CuO NPs as promising candidate due to low cost, abundant resources, non-toxicity and easy preparation in various shapes of nanosized dimensions. CuO NPs has been widely used in electrochemical cells,[20] gas sensors,[21] photovoltaic cells,[22] thermoelectric materials,[23] nanofluids and for photocatalysis.[24,25] The methods to synthesize CuO nanomaterials are diverse, such as

electrochemical deposition, alcohothermal, solid-state reaction and sol–gel.[26-29] However above mentioned methods for synthesis of CuO NPs had some disadvantage such as time consuming, expensive, pollution causing and low yields. To overcome all the problems we have chosen microwave (MW) synthesis over conventional synthesis. It takes just 4 mins to synthesis CuO NPs of 17-22 nm size. This method is economical both in terms of energy consumption and time.

The purpose of the present work is to explore the utility of CuO NPs as catalyst in synthesis of xanthenes under solvent free conditions. In the present work, CuO NPs are acting as efficient heterogeneous catalyst in synthesis of xanthenes in terms of short reaction time, easy work up, excellent yield, enhanced energy efficiency, cost effective and no harmful by-products

2. Results and Discussion

2.1 Characterization of CuO NPs

Figure 1 displays FTIR spectra of CuO NPs. The broad band at 3200 cm^{-1} and small band at 1637 cm^{-1} correspond to the physical adsorbed water on the sample. The absorbance band at 1637 cm^{-1} is due to bending vibration involved in H-O-H angle and 3200 cm^{-1} band is due to stretching vibration of O-H bond.[30] Absorption band between 417 cm^{-1} and 1030 cm^{-1} was attributed to the asymmetric and symmetric stretching frequency of Cu-O-Cu vibrational bands respectively.[31] All the FTIR peaks of CuO NPs were slightly shifted to higher frequency than that of bulk CuO, which indicates the formation of small sized particles. Further, all the peaks of CuO NPs were relatively broad, which represent more symmetrical structure.

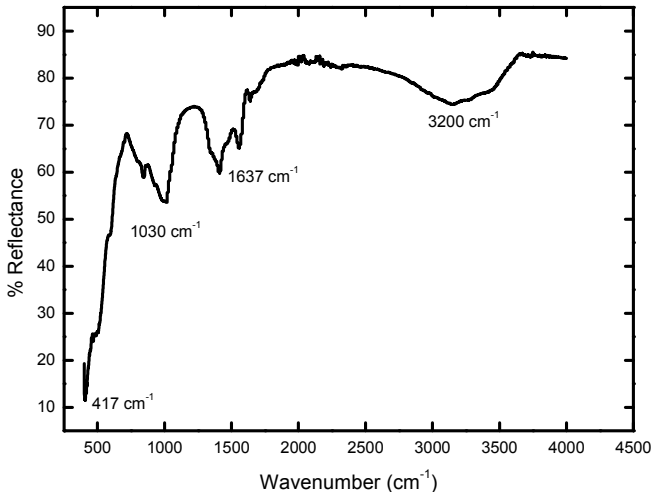

Fig. 1 FTIR spectra of CuO NPs

XRD is powerful technique to analyze the structure of the material and weather the substance is crystalline or amorphous, as for crystalline substance well defined peaks are observed in XRD. Diffraction peaks for CuO NPs were obtained with (hkl) values as (110), (-111), (111/ 200), (-202), (020), (202), (-113), (022/ -311), (113/220), (311), (004/-222) which are found to be same for single phase CuO NPs with a monoclinic (card JCPDS 72-0629)[32] as shown in Fig. 2. No peaks of impurity was found in XRD pattern. Particle size was calculated from FWHM of reflection (111/200) of monoclinic CuO structure using Debye Scherrer formula (Eq.1). The particle size was found to be ~18 nm.

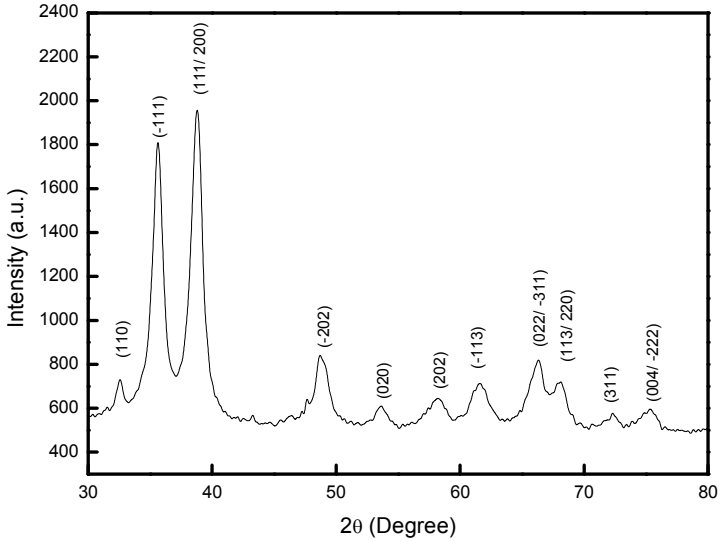

Fig. 2 XRD of CuO NPs

For determining the morphology, TEM micrograph of CuO NPs was taken. As illustrated from the Fig. 3, NPs were almost spherical in shape, well dispersed and narrow range of size distribution (17 – 22 nm).

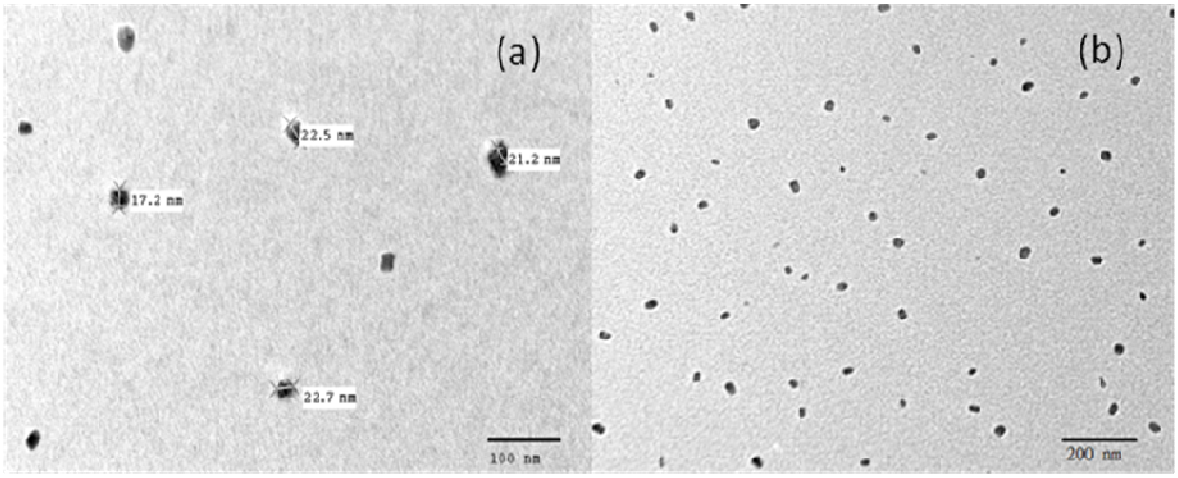

Fig. 3 TEM micrograph of CuO NPs (a) at higher magnification (b) at low magnification

The particle size distribution of synthesized CuO NPs has been estimated by particle size analyzer (PSA). Fig. 4 shows the typical particle size distribution graph which reveals that the average diameter of synthesized CuO NPs is 25 nm. The polydispersity index (PDI) of synthesized nanoparticles is found to be 0.20 that confirms the monodispersity of synthesized NPs.

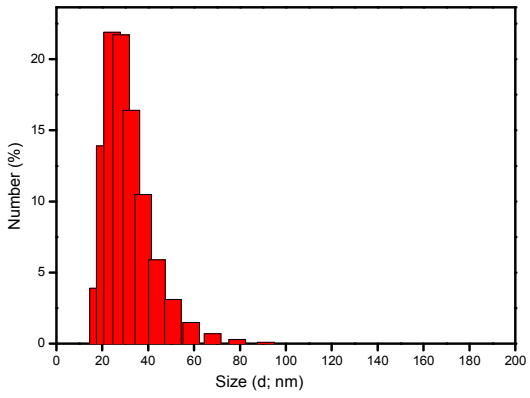

Fig. 4 particle size distribution obtained from particle size analyzer of CuO NPs

2.2 Catalytic activity towards synthesis of Xanthenes

2.2.1 Variation of amount of catalyst

Synthesis of xanthenes have been chosen as a model reaction to test the catalytic activity of CuO nanoparticles. Initially, in order to optimization of the reaction conditions, we have considered the reaction of napthol and bezaldehyde in a 2:1 ratio as a model substrate in the presence of CuO NPs as catalyst under solvent free conditions at 80^{o}C as a heterogeneous catalyst (Scheme 1). The results in Table 1 confirm that the yield of 5a xanthenes increased with increase in the amount of catalyst from 2 mg to 7 mg. Further increase in the amount of catalyst showed no improvement in yield.

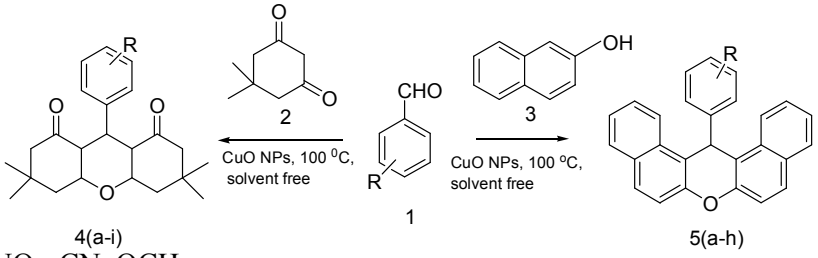

R= H, Cl, Br, NO_2, CN, OCH_3

Scheme 1 Synthesis of xanthenes using CuO NPs as catalyst

Table 1. Variation of amount of catalyst for 5a in table 2

S.No.	Amount of catalyst (mg)	Time (mins)/ % yield
1.	nil	60/nil
2.	2	25/60
3.	3	22/68
4.	4	20/72
5.	5	18/80
6.	6	17/95
7.	7	16/95
8.	8	14/89
9.	8	16/95

2.2.2 Synthesis of different xanthenes (Products)

After optimization of the reaction conditions, the reaction of β-naphthol or dimedone with several aldehydes with electron withdrawing and electron releasing group were carried out in the presence of CuO NPs according to the general experimental procedure. In all cases, the two component reaction proceeded smoothly to give corresponding xanthene in moderate to good yields (Table 2).

Table 2. Synthesis of different xanthenes using CuO NPs

S.No.	Benzaldehyde	Product (xanthenes)	Time (mins)	Yield (%)	Melting point	Ref.
4a	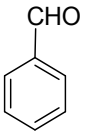	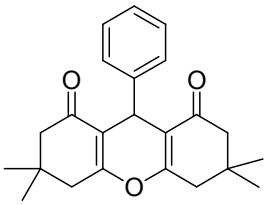	14	89	202-204	42
4b	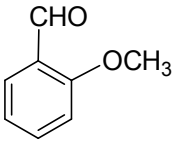	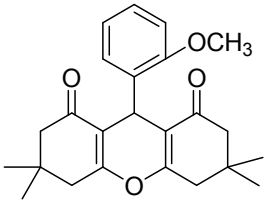	18	92	230-231	42
4c	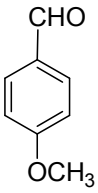	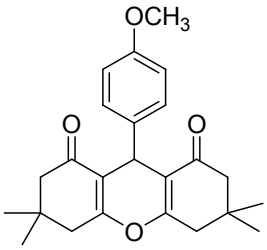	15	87	241-243	40
4d	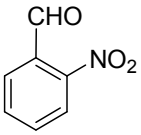	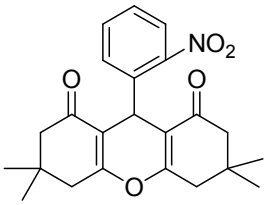	9	90	219-221	42
4e	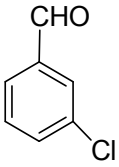	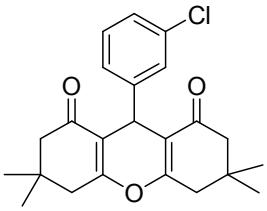	12	89	183-184	40
4f	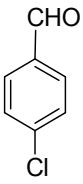	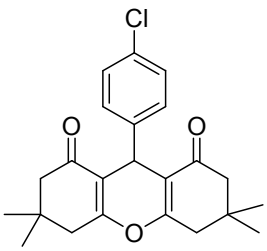	13	90	230-232	40
4g	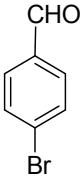	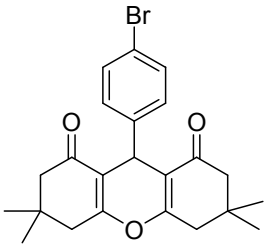	13	89	240-241	40

4h	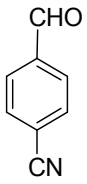	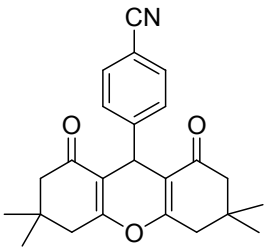	9	95	261-262	40
4i	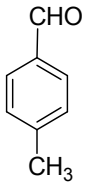	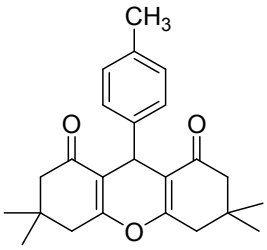	20	85	214-215	40
5a	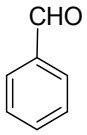	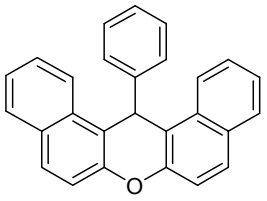	16	95	181-183	40
5b	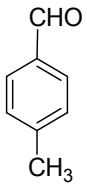	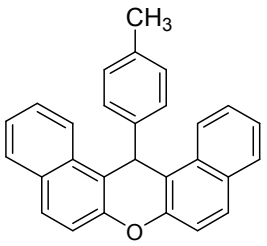	23	84	227-229	40
5c	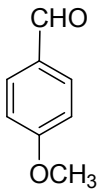	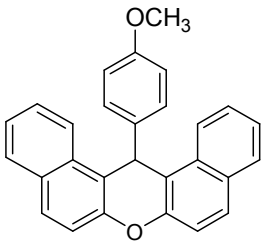	25	82	203-204	40
5d	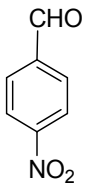	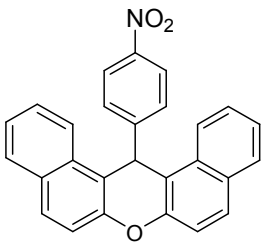	14	93	310-312	40
5e	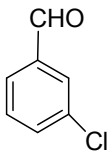	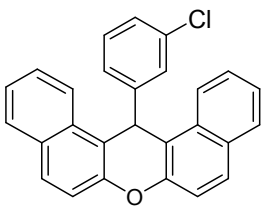	15	86	211-212	42

5f	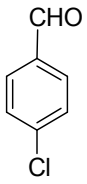	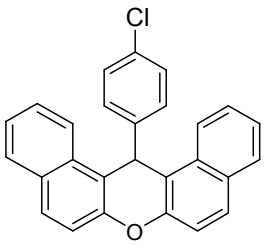	15	83	287-289	40
5g	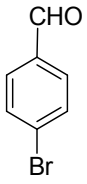	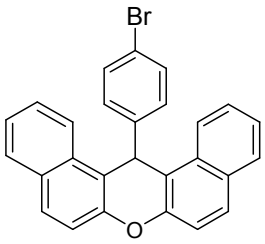	16	87	296-297	40
5h	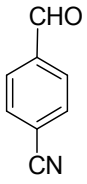	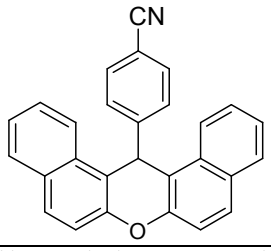	13	90	218-219	40

Their melting points are compared with reported values. Amount catalyst used was 7 mg.

2.2.3 Recyclability of catalyst

Recyclability of the catalyst was assessed by using it for 4 cycles. Figure 5 depicts that insignificant decrease in yield of product was obtained even at 4th recycle. To find out why there is decrease in activity of used CuO NPs after 4 cycle, the recycled CuO NPs has been characterized by TEM [Fig. S1 Supporting information]. As these recycled CuO NPs form clusters so surface to volume ratio decreases and their activity also decreases.

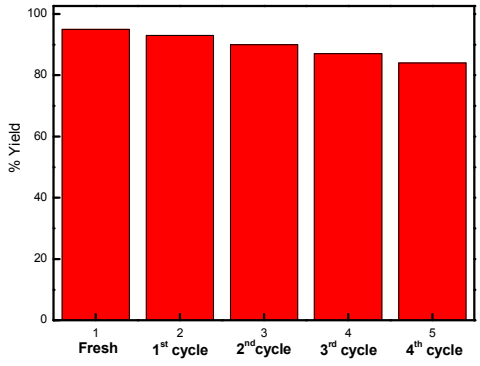

Fig. 5 Recycling ability of CuO NPs for 5a in table 2

2.3 Comparison with other catalyst present in literature

Earlier work[18, 19, 36-43] carried out for synthesis of xanthenes showed that reactions with different catalysts required either higher amount of catalyst or longer reaction time. In some cases reactions were performed in di chloro methane (DCM) which results in difficult work up and environment hazards. A comparison of the use of CuO NPs in present work with some of the other reported catalysts for synthesis of xanthenes has been listed in Table 3. As evident from the table 3 the size of CuO NPs is smaller than the other catalysts viz. ZnO NPs[18] and Fe_3O_4 NPs[19] for the synthesis of xanthenes. These results are in consistent with the fact that smaller the size of nano-catalyst more will be the catalytic activity (Table 3).

Table 3. Comparison of CuO NPs with other catalyst used in literature

Name of Catalyst	Amount of Catalyst (mg)	Time/ yield in (%)	Solvent/ condition	Ref.
$K_5CoW_{12}O_{40}.3H_2O$	64	2 (h)/ 91	Solvent free/ 125 ^{0}C	36
Succinimide-N-sulfonic acid	10	35 (mins)/ 92	Solvent free/ 80 ^{0}C	37
Sulfamic acid:	9.7	8 (h)/ 93	Solvent free/ 125 ^{0}C	38
Tungstophosphoric acid/ zirconia composites	50	1 (h)/ 99	Solvent free/ 130 ^{0}C	39
Iodine	25.38	2.5 (h)/ 90	Solvent free/ 90 ^{0}C	40
$Fe(HSO_4)_3$	35	4 (h)/ 85	DCM	41
Amberlyst-15	10	2 (h)/ 94	Solvent free/ 125 ^{0}C	42
Functionalized mesoporous materials	20	6 (h)/ 80	DCM/ 25 ^{0}C	43
ZnO NPs (24 nm)	10	28 (mins)/ 87	Solvent free/ 80 ^{0}C	18
Fe_3O_4 NPs (40-50 nm)	20	30 (mins)/ 88	Solvent free/ 80 ^{0}C	19
CuO NPs (17-22 nm)	7	16 (mins)/ 95	Solvent free/ 80 ^{0}C	This work

2.4 Plausible reaction mechanism

Copper site in CuO NPs behaves as lewis acid, they have great tendency to co-ordinate with different functional group such as carbonyl (-CO), nitrile (-CN), hydroxyl (-OH), thiol (-SH) etc. As

shown in scheme 2 dimedone or aldehyde undergo chemical adsorption by interaction with acidic surface of metal sites. Because of interaction between the carbonyl group of substrate with CuO NPs, the carbonyl group of aldehyde was activated for nucleophilic attack in next step, leading to speed up the rate of reaction. Finally the product was obtained and the CuO NPs being released for further reactions. Similar mechanism is in case of napthol and aldehyde.

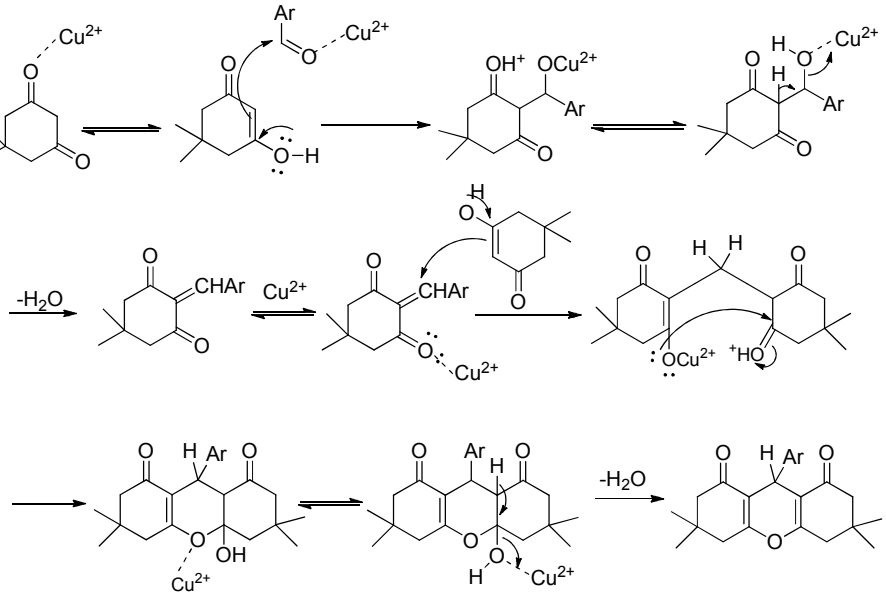

Scheme 2 Plausible mechanism of synthesis of xanthenes

3. Conclusion

CuO NPs have been synthesized in high yield by using water as solvent. Due to the use of high power MW, time taken for synthesis is 4 minutes and the size obtained is also very small (17-22 nm). The as prepared CuO NPs have been employed as a catalyst in the synthesis of xanthenes with varied substitution pattern using conventional heating source under solvent free conditions. It has proved to be very efficient as compared to other catalysts that have already been used for the synthesis of xanthenes. Attractive features such as reduced reaction time, higher yields, ease of product isolation, economic availability of catalyst, simple procedure and solvent free condition combined with easy recovery, no harmful byproduct and

reuse of this catalyst 4 times without much effect in product yield, makes it one of the best catalysts for synthesis of xanthenes.

4. Experimental

4.1 General remarks

X-Ray diffraction (XRD) spectra were recorded on Panalytical X'Pert Pro X-ray diffractrometer equipped with Cu-kα radiation (1.5406 Å) operating at 40 kV, with scanning speed of 8°/min to examine the crystalline phase of the sample. Size is calculated by using Debye Scherrer equation (eq. 1)

$$D = \frac{K\lambda}{\beta Cos\ \theta} \qquad \text{(eq. 1)}$$

where K is shape factor, λ is the X ray wavelength, β is the full width at half the maximum intensity (FWHM), θ is Braggs angle and D is the mean size of particle. Fourier transform infrared (FTIR) spectra was obtained on a Perkin Elmer FTIR spectrophotometer in the frequency range of 4000-1000 cm^{-1} using KBr plates with 100 number scans and 4 cm^{-1} spectral resolution. Transmission electron microscope (TEM) micrograph was obtained by analyzed using Hitachi (H-7500) electron microscope operating at 80 kV. To check the particle size distribution, particle size analyser (PSA) was performed using Malvern Zetasizer nanoseries (Nano-S90). ^{1}H and ^{13}C NMR spectra were measured on a model advance II (Bruker) instrument with frequency 300 MHz for ^{1}H NMR and 100 MHz frequency for ^{13}C NMR using TMS as the internal standard and $CDCl_3$ as solvent. Microwave IFB 20PG2S, with power output-800 watt, operational frequency-2450 MHz has been used for synthesis of CuO NPs.

Dimedone and napthol was supplied by Sigma Aldrich, copper chloride was obtained from Glaxo laboratory India and sodium hydroxide (NaOH) and benzaldehyde was supplied by Qualigens. p-chlorobenzaldehyde, m-chlorobenzaldehyde, o-anisaldehyde, p-anisaldehyde, o-

nitrobenzaldehyde and p-nitrobenzaldehyde, m-nitrobenzaldehyde, p-bromobenzaldehyde, p-cyanobenzaldehyde, p-methyl benzaldehyde were purchased from HiMedia. Ethanol was supplied by Changshu, Yangyuan Chemicals China. Purity of all chemicals was more than 98% and was used without further purification. Doubly distilled water was used for the synthesis of CuO NPs.

4.2 Preparation of CuO NPs

In a typical reaction, 100 ml of 0.01 M solution of $CuCl_2.2H_2O$ and 100 ml of 0.03 M solution of NaOH was prepared. Both the prepared solutions were mixed together and microwaved for 4 minutes. The formation of brown precipitates appeared. The final product was separated out by filteration, washed with distilled water and dried under room temperature. To optimise the synthesis, we have changed reaction time and found that there was no complete conversion of reactant into product before 4 minutes as peaks of impurities were obtained in XRD [Fig. S2 Supporting information]. These impurity peaks are labelled as 1 and 2 in Fig. S2 Supporting information, which are due to monoclinic phase of $Cu_2(OH)_3Cl$.[44] To verify the reproducibility of synthesis of CuO NPs by MW, we have performed the synthesis of NPs three times at the interval of 24 hours. XRD results for the three samples are reproducible with almost same size [Fig. S3 Supporting information].

4.3 Synthesis of Xanthenes

A mixture of aldehyde (1 mmol), 2-naphthol (2 mmol) or dimedone (2 mmol) and CuO NPs (0.007 g) was heated with stirring at 100 °C in an oil bath. The progress of reaction was monitored by TLC. After cooling, the reaction mixture was dissolved in dichloromethane (DCM) and the mixture stirred for 5 min. The suspended solution was filtered and then heterogeneous nanocatalyst was recovered. The dichloromethane was evaporated and the crude product was recrystallized from ethanol to give the pure product. The isolated catalyst

was washed with ethanol and dried at room temperature for over night, catalyst was reused at least 4 times without an appreciable decrease of yield. All of the pure products were characterized by comparison of their physical (melting point) and spectral data (^{1}H and ^{13}C NMR) with those of authentic samples. [33-35] Also the flash chromatography has been done to purify the products by using elutant (ethylacetate/ hexane in ratio 4:6). It has been seen that product got by recrystallization and flash chromatography results came out to be same in terms of yield and purity (^{1}H NMR) [Fig. S4 Supporting information].

Characterization of Xanthenes

Table 2, 4a; ^{1}H NMR (300 MHz, $CDCl_3$); δ_H (ppm): 0.97 (6H, s, 2× CH_3), 1.08 (6H, s, 2× CH_3), 2.16-2.18 (4H, d, 2× CH_2), 2.44 (4H, d, 2× CH_2), 4.71 (1H, s, CH), 7.01-7.26 (6H, m). ^{13}C NMR (100 MHz, $CDCl_3$); δ_C (ppm): 27.37, 29.33, 31.82, 32.19, 40.93, 50.75, 115.76, 126.39, 128.04, 128.38, 144.04, 162.01, 195.96

Table 2, 4b; ^{1}H NMR (300 MHz, $CDCl_3$); δ_H (ppm): 0.85 (6H, s, 2× CH_3), 1.00 (6H, s, 2× CH_3), 1.97-2.10 (4H, q, 2× CH_2), 2.21-2.37 (4H, q, 2× CH_2), 3.67 (1H, s, OCH_3), 4.70 (1H, s, CH), 6.60-7.26 (4H, m, Ar-H). ^{13}C NMR (100 MHz, $CDCl_3$); δ_C (ppm): 26.89, 29.37, 29.63, 32.10, 41.06, 50.75, 55.11, 110.60, 113.95, 120.48, 127.77, 130.52, 132.21, 157.53, 162.21, 195.45

Table 2, 4c; ^{1}H NMR (300 MHz, $CDCl_3$); δ_H (ppm): 0.97 (6H, s, 2× CH_3), 1.08 (6H, s, 2× CH_3), 2.10-2.17 (4H, q, 2× CH_2), 2.40-2.42 (4H, q, 2× CH_2), 3.70 (3H, s, OCH_3), 4.65 (1H, s, CH), 6.69-7.17 (4H, dd, Ar-H). ^{13}C NMR (300 MHz, $CDCl_3$); δ_C (ppm): 27.40, 29.35, 30.96, 32.20, 40.93, 50.78, 55.02, 113.50, 115.90, 129.31, 136.42, 158.03, 161.83, 196.10

Table 2, 4d; ^{1}H NMR (300 MHz, $CDCl_3$); δ_H (ppm): 0.98 (6H, s, 2× CH_3), 1.11 (6H, s, 2× CH_3), 2.10-2.24 (4H, q, 2× CH_2), 2.46 (4H, s, 2× CH_2), 4.76 (1H, s, CH), 7.41-8.08 (4H, dd,

Ar-H). ^{13}C NMR (100 MHz, $CDCl_3$); δ_C (ppm): 27.41, 29.42, 32.30, 40.99, 50.61, 114.75, 123.44, 129.39, 146.71, 151.23, 162.45, 195.43

Table2, 4e; ^{1}H NMR (300 MHz, $CDCl_3$); δ_H (ppm): 0.86 (6H, s, 2× CH_3), 0.99 (6H, s, 2× CH_3), 2.04-2.06 (4H, q, 2× CH_2), 4.59 (1H, s, CH), 7.24-7.39 (4H, m, Ar-H). ^{13}C NMR (100 MHz, $CDCl_3$); δ_C (ppm): 27.43, 29.44, 32.28, 32.52, 41.00, 50.63, 114.84, 129.35, 131.95, 162.37, 195.42.

Table 2, 4f; ^{1}H NMR (300 MHz, $CDCl_3$); δ_H (ppm): 0.93 (6H, s, 2×CH_3), 1.06 (6H, s, 2×CH_3), 2.10-2.11 (4H, q, 2× CH_2), 2.37 (4H, s, 2× CH_2), 4.57 (1H, s, CH), 7.05-7.08 (2H, d, Ar-H), 7.23-7.26 (2H, d, Ar-H).^{13}C NMR (100 MHz, $CDCl_3$); δ_C (ppm): 27.50, 29.52, 31.58, 32,27, 41.04, 50.70, 115.45, 120.49, 130.24, 131.22, 143.07, 161.77,195.10

Table 2, 4g; ^{1}H NMR (300 MHz, $CDCl_3$); δ_H (ppm): 0.97 (6H, s, 2×CH_3), 1.09 (6H, s, 2× CH_3), 2.13 2.15 (4H, q, 2× CH_2), 2.40-2.41 (4H, s, 2× CH_2), 4.62 (1H, s, CH), 7.13-7.15 (4H, m , Ar-H). ^{13}C NMR (300 MHz, $CDCl_3$); δ_C (ppm): 27.49, 29.53, 31.48, 32.27, 41.04, 50.70, 115.53, 128.29, 129.84, 132.31, 142.54, 161.75, 195.12

Table 2, 4h; ^{1}H NMR (300 MHz, $CDCl_3$); δ_H (ppm): 1.03 (6H, s, 2× CH_3), 1.13 (6H, s, 2× CH_3), 2.20-2.21 (4H, q, 2× CH_2), 2.47 (4H, q, 2× CH_2), 4.69 (1H, s, CH), 7.09-7.27 (4H, m, Ar-H). ^{13}C NMR (100 MHz, $CDCl_3$; δ_C (ppm): 27.51, 29.41, 31.75, 32.29, 41.00, 50.72, 115.30, 126.80, 127.15, 128.25, 129.24, 134.04, 146.04, 162.08, 195.45

Table 2, 4i; ^{1}H NMR (300 MHz, $CDCl_3$); δ_H (ppm): 1.04 (6H, s, 2× CH_3), 1.10 (6H, s, 2× CH_3), 2.14-2.15 (4H, d), 2.24 (3H, s, CH_3), 2.29 2.41 (4H, d), 4.62 (1H, s, CH), 6.94-6.97 (2H, d, Ar-H), 7.08 7.10 (2H, d, Ar-H). ^{13}C NMR (100 MHz, $CDCl_3$); δ_C (ppm): 27.55, 29.61, 31.46, 32.30, 41.09, 50.80, 51.12, 116.07, 128.39, 128.86, 135.59, 141.15, 161.37, 163.06, 195.18

Table 2, 5a; ^{1}H NMR (300 MHz, $CDCl_3$); δ_H (ppm): 6.44 (1H, s, CH), 7.24 (2H, s, Ar-H), 7.37-7.50 (9H, m), 7.74-7.79 (4H, m), 8.33-8.36 (2H, d, Ar-H). ^{13}C NMR(100 MHz, $CDCl_3$); δ_C (ppm): 38.10, 117.39, 118.05, 122.73, 124.22, 126.77, 128.26, 128.54, 128.85, 131.14, 131.58, 145.02, 148.80

Table 2, 5b; ^{1}H NMR (300 MHz, $CDCl_3$); δ_H (ppm): 2.12 (3H, s, CH_3), 6.39 (1H, s, CH), 6.90-6.93 (2H, d. Ar-H), 7.33-7.38 (4H, m), 7.43-7.46 (2H, d, Ar-H), 7.50-7.53 (2H, d, Ar-H), 7.55-7.78 (4H, m), 8.32-8.35 (2H, d, Ar-H). ^{13}C NMR (100 MHz, $CDCl_3$); δ_C (ppm): 21.02, 37.72, 117.50, 118.03, 122.79, 124.17, 126.71, 128.13, 128.74, 128.82, 129.25, 131.16, 131.59, 135.67, 142.18, 148.72

Table 2, 5c; ; ^{1}H NMR (300 MHz, $CDCl_3$); δ_H (ppm): 3.54 (3H, s, OCH_3), 6.37 (1H, s, CH), 6.58-6.60 (2H, d, Ar-H), 7.30-7.35 (4H, m), 7.38-7.40 (2H, d, Ar-H), 7.47-7.51 (2H, t, Ar-H), 7.69-7.75 (4H, m), 8.29-8.31 (2H, d, Ar-H). ^{13}C NMR (100 MHz, $CDCl_3$); δ_C (ppm): 37.08, 55.05, 113.84, 117.53, 117.99, 122.67, 124.19, 126.74, 128.70, 128.78, 129.13, 131.07, 131.41, 148.69, 157.84

Table 2, 5d; ^{1}H NMR (300 MHz, $CDCl_3$); δ_H (ppm): 6.53 (1H, s, CH), 7.34-7.38 (2H, t, Ar-H), 7.42-7.44 (2H, d, Ar-H), 7.50-7.54 (2H, t, Ar-H), 7.59-7.62 (2H, d, Ar-H), 7.75-7.79 (4H, m), 7.91-7.93 (2H, d, Ar-H), 8.19-8.22 (2H, d, Ar-H). ^{13}C NMR (100 MHz, $CDCl_3$); δ_C (ppm): 37.86, 115.78, 118.06, 122.03, 123.86, 124.58, 127.19, 128.96, 129.06, 129.60, 131.09

Table 2, 5e; ^{1}H NMR (300 MHz. $CDCl_3$); δ_H (ppm): 6.36 (1H, s, CH), 6.85-6.88 (1H, d), 6.95-6.99 (1H, t), 7.30-7.40 (6H, m), 7.47-7.51 (2H, t), 7.69-7.71 (4H, m), 8.21-8.23 (2H, d, Ar-H). ^{13}C NMR (100 MHz, $CDCl_3$); δ_C (ppm): 37.75, 116.58, 118.08, 122.40, 124.38, 126.40, 126.74, 126.96, 128.33, 128.90, 129.16, 129.60, 131.06, 131.27, 134.42, 146.88, 148.79

Table 2, 5f; ^{1}H NMR (300 MHz, $CDCl_3$); δ_H (ppm): 6.46 (1H, s, CH), 7.08-7.10(2H, d, Ar-H), 7.39-7.48 (8H, m), 7.78-7.83 (4H,m) 8.29-8.32 (2H,d, Ar-H). ^{13}C NMR (100 MHz, $CDCl_3$); δ_C (ppm): 37.37, 116.76, 118.01, 122.40, 124.36, 126.91, 128.63, 128.90, 129.08, 129.48, 131.08, 131.26, 132.09, 143.45, 148.72

Table 2, 5g; ^{1}H NMR (300 MHz, $CDCl_3$); δ_H (ppm): 5.21 (1H, s, CH), 7.16-7.18 (2H, d, Ar-H), 7.29-7.40 (6H, m), 7.48-7.52 (2H, t, Ar-H), 7.71-7.76(4H, m), 8.22-8.24 (2H, d, Ar-H). ^{13}C NMR (100 MHz, $CDCl_3$); δ_C (ppm): 37.72, 115.89, 118.12, 121.69, 122.02, 122.71, 124.58, 127.24, 129.06, 129.49, 129.56, 131.04, 131.06, 134.2

Table 2, 5h; ^{1}H NMR (300 MHz, $CDCl_3$); δ_H (ppm): 6.57 (1H, s, CH), 7.44-7.48 (4H, m), 7.50-7.53 (2H, d, Ar-H), 7.59-7.65 (4H, m), 7.84-7.88 (4H, m), 8.28-8.30 (2H, d, Ar-H). ^{13}C NMR (100 MHz, $CDCl_3$); δ_C (ppm): 26.03, 122.09, 124.65, 127.24, 128.92, 129.21, 129.66, 155.58

Acknowledgements

GRC would like to acknowledge the financial support of the SERB-DST India (SB/EMEQ-166/2013) and PB is thankful to UGC, Delhi for the fellowships

References

1 A. S. Roy, J. Mondal, B. Banerjee, P. Mondal, A. Bhaumik and Sk. M. Islam, *Appl. Catal. A*, 2014, **469**, 320-327.

2 G. R. Chaudhary, P. Bansal and S. K. Mehta, *Chem. Eng. J.*, 2014, **243**, 217-224.

3 E. Y. Yuzik-Klimova, N. V. Kuchkina, S. Sorokina, D. G. Morgan, L. Z. Nikoshvili, N. Lyubimova, V. G. Matveeva, E. M. Sulman, B. D. Stein, W. E. Mahmoud, A. A. Al-Ghamdi, A. Kostopoulou, A. Lappas, Z. B. Shifrina and L. M. Bronstein, *RSC Adv.*, 2014, DOI: 10.1039/C4RA00878B.

4 M. Tajbakhsh, M. Farhang, R. Hosseinzadeh and Y. Sarrafi, *RSC Adv.*, 2014, DOI: 10.1039/C4RA03333G

5 A. Pramanik, S. Pathak, K. Debnath and M. R. Mollick, *RSC Adv.*, 2014, DOI: 10.1039/C4RA03384A

6 F. Shirini, A. Yahyazadeh and K. Mohammadi, *Chinese Chem. Lett.*, 2014, **25**, 341-347.

7 H. Naeimi and Z. S. Nazifi, *Appl. Catal. A*, 2014, **477**, 132-140.

8 M. Mokhtary and S. Refahati, *Dyes and Pigments*, 2013, **99**, 378-381.

9 J. M. Khurana, D. Magoo, K. Aggarwal, N. Aggarwal, R. Kumar and C. Srivastava, *Eur. J. Med. Chem.*, 2012, **58**, 470-477.

10 W. Zhang and R. Xu, *Int. J. Hydrogen Energy*, 2012, **37**, 17899-17909.

11 A. Ojida, I. Takashima, T. Kohira, H. Nonaka and I. Hamachi, *J. Am. Chem. Soc.*, 2008, **130**, 12095-12101.

12 H. N. Hafez, M. I. Hegab, I. S. Ahmed-Farag and A. B. A. El-Gazzar, *Bioorg. Med. Chem. Lett.*, 2008, **18**, 4538-4543.

13 J. P. Tardivoa, A. D. Giglio, C. S. de Oliveirab, D. S. Gabrielli, H. C. Junqueirab, D. B. Tadab, D. Severinob, R. deF. Turchiello and M. S. Baptista, *Photodiagn. Photodyn. Ther.* 2005, **2**, 175-191.

14 K. R. Moghadam and S. C. Azimi, *J. Mol. Catal. A*, 2012, **363-364**, 465-469.

15 A. Zare, A. R. Moosavi-Zare , M. Merajoddin, M. A. Zolfigol, T. Hekmat-Zadeh, A. Hasaninejad, A. Khazaei, M. Mokhlesi, V. Khakyzadeh, F. Derakhshan-Panah, M. H.Beyzavi , E. Rostami , A. Arghoon and R. Roohandeh, *J. Mol. Liq.*, 2012, **167**, 69-77.

16 M. Mokhtary and S. Refahati, *Dyes and Pigments*, 2013, **99**, 378-381.

17 N. G. Khaligh, *Ultrason. Sonochem.*, 2012, **19**, 736-739.

18 J. Safaei-Ghomi and M. A. Ghasemzadeh, *Chinese Chem. Lett.*, 2012, **23**, 1225-1229.

19 M. A. Ghasemzadeh, J. Safaei-Ghomi and S. Zahedi, J. Serb. Chem. Soc. 2013, **6**, 769-779

20 M. Kong, W. Zhang, Z. Yang, S. Weng and Z. Chen, *Appl. Surf. Sci.* 2011, **258**, 1317-1321.

21 C. Yang, X. Su, J. Wang, X. Cao, S. Wang and L. Zhang, *Sensor Actuat. B Chem.*, 2013, **185**, 159-165.

22 C. C. Vidyasagar, Y. A. Naik, T. G. Venkatesh and R. Viswanatha, *Powder Technol.*, 2011, **214**, 337-343.

23 Q. Zhang, K. Zhang, D. Xu, G. Yang, H. Huang, F. Nie, C. Liu and S. Yang, *Prog. Mater Sci.*, 2014, **60**, 208-337.

24 M. M. Sarafraz and F. Hormozi, *Exp. Therm Fluid Sci.*, 2014, **52**, 205-214.

25 A. N. Ejhieha and M. K. Shamsabadi, *Appl. Catal. A Gen.*, 2014, **477**, 83-92.

26 N. Mukherjee, B. Show, S. K. Maji, U. Madhu, S. K. Bhar, B. C. Mitra, G. G. Khan and A. Mondal, *Mater. Lett.*, 2011, **65**, 3248-3250.

27 Z. Hong, Y. Cao and J. Deng, *Mater. Lett.*, 2002, **52**, 34-38.

28 S. Sohrabnezhad and A. Valipour, *Spectrochim. Acta A*, 2013, **114**, 298-302.

29 J. Jayaprakash, N. Srinivasan and P. Chandrasekaran, *Spectrochim. Acta A*, 2014, **123**, 363-368.

30 S. Y. Venyaminov and F. G. Prendergast, *Analytical Biochemistry*, 1997, **248,** 234-245.

31 B. Zhao, P. Liu, H. Zhuang, Z. Jiao, T. Fang, W. Xu, B. Lub and Y. Jiang, *J. Mater. Chem. A*, 2013, **1**, 367-373.

32 D. Han, H. Yang, C. Zhu and F. Wang, *Powder Technol.*, 2008, **185**, 286-290.

33 J. Safaei-Ghomi and M. A. Ghasemzadeh, *Chinese Chem. Lett.*, 2012, **23**, 1225-1229.

34 J. Safaei-Ghomi and M. A. Ghasemzadeh, J. Saudi Chem. Soc., 2012, dx.doi.org/10.1016/j.jscs.2012.05.007.

35 B. Karami, S. J. Hoseini, K. Eskandari, A. Ghasemi and H. Nasrabadi, *Catal. Sci. Technol.*, 2012, **2**, 331-338.

36 L. Nagarapu, S. Kantevari, V. C. Mahankhali and S. Apuri, *Catal. Comm.*, 2007, **8**, 1173-1177.

37 F. Shirini and N. G. Khaligh, *Dyes and Pigments*, 2012, **95**, 789-794.

38 B. Rajitha, B. S. Kumar, Y. T. Reddy, P. N. Reddy and N. Sreenivasulu, *Tetrahedron Lett.*, 2005, **46**, 8691-8693.

39 T. S. Rivera, A. Sosa, G. P. Romanelli, M. N. Blanco and L. R. Pizzio, *Appl. Catal. A Gen.*, 2012, **443-444**, 207-213.

40 B. Das, B. Ravikanth, R. Ramu, K. Laxminarayana and B. V. Rao, *J. Mol. Catal. A Chem.*, 2006, **255**, 74-77.

41 H. Eshghi, M. Bakavoli and H. Moradi, *Chinese Chem. Lett.*, 2008, **19**, 1423-1426.

42 S. Ko and C. Yao, *Tetrahedron Lett.*, 2006, **47**, 8827-8829.

43 J. Mondal, M. Nandi, A. Modak and A. Bhaumik, *J. Mol. Catal. A Chem.*, 2012, **363-364**, 254-264.

44 A. Pendashteh, M. S. Rahmanifar and M. F. Mousavi, *Ultrason. Sonochem.*, 2014, **21**, 643-652

Table of contents entry

GRAPHICAL ABSTRACT

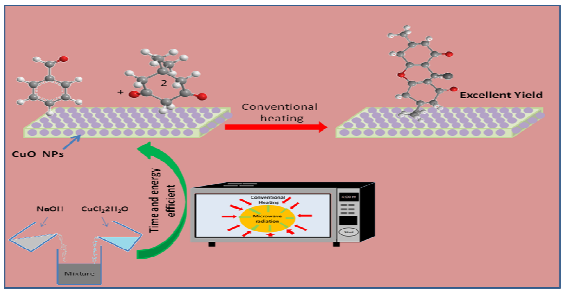

CuO nanoparticles synthesized *via* cost-effective and greener-approach. CuO Nanoparticles were used first time as catalyst in synthesis of xanthenes that proved to be efficient as compared to other catalysts.